INT. J. REMOTE SENSING, 2002, VOL. 23, NO. 10, 1985–2004

Taylor & Francis
Taylor & Francis Group

Monitoring land-use change in the Pearl River Delta using Landsat TM

K. C. SETO*†, C. E. WOODCOCK†, C. SONG†, X. HUANG‡, J. LU§ and R. K. KAUFMANN†

†Department of Geography, Boston University Boston, Massachusetts 02215, USA
‡Institute of Remote Sensing Applications, Chinese Academy of Sciences, Beijing, 100101 China
§Institute of Geography, Chinese Academy of Sciences, Beijing, 100101 China

(*Received 18 October 1999; in final form 12 December 2000*)

Abstract. The Pearl River Delta in the People's Republic of China is experiencing rapid rates of economic growth. Government directives in the late 1970s and early 1980s spurred economic development that has led to widespread land conversion. In this study, we monitor land-use through a nested hierarchy of land-cover. Change vectors of Tasseled Cap brightness, greenness and wetness of Landsat Thematic Mapper (TM) images are combined with the brightness, greenness, wetness values from the initial date of imagery to map four stable classes and five changes classes. Most of the land-use change is conversion from agricultural land to urban areas. Results indicate that urban areas have increased by more than 300% between 1988 and 1996. Field assessments confirm a high overall accuracy of the land-use change map (93.5%) and support the use of change vectors and multidate Landsat TM imagery to monitor land-use change. Results confirm the importance of field-based accuracy assessment to identify problems in a land-use map and to improve area estimates for each class.

1. Introduction

The Pearl River (Zhujiang) Delta in the Guangdong Province is one of the fastest developing regions in China. Between 1985 and 1997, the Province's GDP grew at an average annual rate of 15.3% (Guangdong Statistical Bureau 1998). Two driving forces spur this rapid rate. First, the establishment of Special Economic Zones (SEZs) in the Guangdong Province by the China National People's Congress have opened the doors to trade and commerce from abroad. The purposes of SEZs are: (1) to attract foreign investment, (2) to test and evaluate different economic policies, and (3) to increase exports (Wu 1989, Ning 1991, Chu 1998). Secondly, and perhaps equally important to the development of the Delta, is its proximity to Hong Kong and the cultural ties to overseas Chinese investors. Foreign direct investment in Guangdong comes largely from overseas Chinese investors in Hong Kong, Taiwan, Singapore and the USA. Relative to Hong Kong, land rents and labour in China

*Present address: Center for Environmental Science and Policy, Stanford University, Stanford, California 94305-6055, USA; e-mail: kseto@stanford.edu

International Journal of Remote Sensing
ISSN 0143-1161 print/ISSN 1366-5901 online © 2002 Taylor & Francis Ltd
http://www.tandf.co.uk/journals
DOI: 10.1080/01431160110075532

are inexpensive, and SEZs have accelerated the migration of businesses and light industry across the border.

Rapid rates of economic development have had myriad impacts on the residents and the landscape. Most evidently for residents, economic development has increased per capita income, which has increased the ownership of private vehicles and homes. From 1994 to 1997, the number of motor vehicles in the provincial capital, Guangzhou, increased by 45% and the amount of living space per capita has more than doubled between 1980 and 1997 (Guangdong Statistical Bureau various years). In China, as in most developing countries, a rise in income leads to an increase in the consumption of luxury goods such as meat products (Sicular 1985). This increased demand for meat often accompanies an increase in basic dietary standards, raising the demand for grain production both for direct consumption and for livestock feed. The rise in grain demand can be met by expanding or intensifying production. The possibility of expanding production is constrained in the Pearl River Delta by the increasing demand for space by a burgeoning transportation network and residential, industrial and commercial construction. The net effect is a reduction in the amount of land available for agricultural production.

Between 1979–81 and 1989–91, approximately 4% of total cropland and 6.5% of total forest cover in China were converted for other uses. The Chinese Academy of Sciences estimates that 333 000 ha of farmland are converted to industrial, commercial and residential uses each year (World Resources Institute 1994). Others estimate that economic activity in the 1990s will result in the conversion of 3 to 6 million ha of agricultural land into urban areas (Smil 1993). A recent study indicates that development has spurred accelerated land conversion in one county of the Guangdong Province (Li and Yeh 1998). However, reliable area estimates of land-use change for a large part of the Delta are not available and the driving forces behind the land-use conversions are not well understood. Official statistics on cultivated land and land-use are probably biased due to tendencies to overestimate production and underestimate the amount of cultivated land (Smil 1995).

To understand the socio-economic driving forces behind land-use change, we are engaged in a two-part effort to: (1) estimate land-use change over time for a cross-section of counties in the Pearl River Delta, and (2) incorporate the area estimates in a socio-economic analysis of the factors that influence land-use change. Specifically, we are interested in the rates of conversion of lands to more intensive uses, such as the conversion of natural vegetation or agricultural lands to urban land-uses. The purpose of this paper is to report on our efforts to provide estimates of land-use change between 1988 and 1996 in the Pearl River Delta using Landsat Thematic Mapper (TM) imagery.

2. Land-use versus land-cover change

Satellite imagery has been well utilized in the natural science communities for measuring qualitative and quantitative terrestrial land-cover changes (Coppin and Bauer 1994, Collins and Woodcock 1996, Gopal and Woodcock 1996, Pax Lenney *et al.* 1996). Qualitative changes in landscapes occur either as natural phenomena (wildfires, lightning strikes, storms, pests) or can be human induced (selective logging, agroforestry). Quantitative land-cover change is the wholesale categorical transformation of the land, and although it can occur as a natural phenomenon as caused by fires and storms, large-scale replacement of one land-cover type by another is usually induced by human activity (forest clearing, agricultural expansion, urban

growth). Both qualitative and quantitative changes in land-cover have been successfully monitored with remote sensing, with research dominated by efforts at monitoring change in vegetation and forest canopies (Collins and Woodcock 1994, Macleod and Congalton 1998).

More recently, social scientists have begun to use satellite imagery to address issues at the interface of economics, politics and the natural environment. Among these research activities is the attempt to integrate remote sensing with socio-economic data in order to understand the anthropogenic causes of land conversion (Skole *et al.* 1994). However, because satellites observe land-cover and not land-use, the effort to link remotely sensed observations of the landscape with human activity on the ground requires data different from conventional remote sensing studies. For these cross-disciplinary, integrated studies, a core requirement is information on how land is used.

In many remote sensing change detection studies, land-use and land-cover often are used interchangeably (Green *et al.* 1994, Dimyati *et al.* 1996, Heikkonen and Varfis 1998). Land-use often corresponds to a land-cover type and, in these instances, the concepts are synonymous. For example, a pasture is a land-use but also describes the land-cover. Urban areas refer to both a type of land utilization (residential, commercial, industrial, transportation) and a particular land-cover (concrete, steel, brick). In cases like this where there is a direct relational correspondence between land-use and land-cover, the two concepts are essentially identical. However, this direct relationship does not always exist. For these situations, it is important to distinguish land-use from land-cover; the latter measures the physical attributes, condition and characteristics of the Earth's surface, while the former describes how the land-cover is utilized. Particularly for applications that link remote sensing with human activity, this differentiation is important because land-use emphasizes the functional role of land in economic activities (Campbell 1983) while land-cover does not. Therefore confounding land-cover with land-use may generate biased results in these studies.

3. Monitoring urbanization with remote sensing

A number of change detection techniques have been developed over the last 20 years. They include image differencing, image regression, image ratioing, vegetation index differencing, principal component analysis, change vector analysis, post-classification subtraction and vegetation index differencing (Singh 1989). Although these methods have been successful in monitoring change for a myriad of applications, there is no consensus as to a 'best' change detection approach. The type of change detection method employed will largely depend on data availability, the geographic area of study, time and computing constraints, and type of application.

An increase in urban structures and a decrease in vegetation cover usually characterize development. Previous work using TM data to map urban areas had limited success. Although the high spatial resolution of TM allows for better discrimination of urban features such as road networks, the spatial variance for an urban environment is high (Woodcock and Strahler 1987). This heterogeneous nature of urban areas makes it particularly difficult to classify (Haack *et al.* 1987, Khorram *et al.* 1987, Møller-Jensen 1990). Forster (1993) shows that radiometric variation is a function of building size and distribution. In regions of the world where urban features vary significantly by geographic location and access to materials, urban features may be particularly difficult to distinguish. Even with 20 m resolution SPOT

sensor data, Gong and Howarth (1990) had difficulties differentiating between paved surfaces from bare fields and roofs from bare fields. More recently, Heikkonen and Varfis (1998) used neural networks to classify urban areas with high accuracy.

Previous efforts at monitoring urban development utilized the visible red and near-infrared bands to delineate between vegetated and non-vegetated areas. Using Multi-Spectral Scanner (MSS) Band 5 (0.6–0.7 μm) in image differencing, Jensen and Toll (1982) identify urban expansion with 81% accuracy. Their results highlight the importance of incorporating different stages of urban development in the classification scheme. Howarth and Boasson (1983) confirm the use of the MSS red band, and results indicate that image overlay of MSS Band 5 is superior over a Band 5 (red) ratio, Band 7 (near-infrared) ratio and a vegetation index. Fung (1990) reports that one type of image transform may not detect all types of changes. For rural to urban conversions, changes are best detected using multidate Kauth-Thomas change in brightness (ΔB) and image differencing of TM Band 3. Ridd and Liu (1998) propose a chi-squared transformation that detects change from farmland to construction with 87% accuracy and farmland to commercial and industrial areas with 88% accuracy. However, this method is not superior to conventional techniques such as image differencing, image regression or multi-date Tasseled Cap transformation. Li and Yeh (1998) use a multi temporal principal components analysis to monitor urbanization and obtained an overall accuracy of 93%.

Different problems and complexities are presented in monitoring urban development in various parts of the world. In parts of the world where city planners have a model of urban growth, there may be a clear pattern in the development trajectory. In many developing countries, urban development often occurs along the periphery of formal urban planning. Usually, these projects differ in scale and magnitude from their counterparts in developed countries. For example, in developed countries, urban development generally is undertaken by construction firms with mechanized equipment, facilitating the rapid construction of industrial, commercial and residential complexes. In addition, the availability of fossil-fuel powered equipment subsidizes human effort, and the scale of the projects can be large. In China, where labour is abundant and inexpensive, urban development usually occurs with much human effort and with little assistance from motorized equipment. In a place where bricks are laid by hand, the scale of development projects tends to be smaller, and the time horizon for their completion tends to be longer. Therefore, the pattern of urbanization in China may sharply contrast those in industrialized countries.

4. Study area, data and data pre-processing

The study area is the Pearl River Delta in the Guangdong Province of Southern China covered by one Landsat TM scene. The image includes the provincial capital city of Guangzhou and all of the SEZ of Shenzhen, and part of the SEZ of Zhuhai. For this study, we acquired two TM scenes from Landsat World Reference System path 122, row 44 taken on 10 December 1988 and 3 March 1996. Scenes from different seasons were selected because of the limited availability of cloud-free images of the Pearl River Delta.

To compare the satellite images taken from different years and seasons, the images were co-registered to a master image provided by the Institute of Remote Sensing Applications in Beijing. Using nearest neighbour resampling, a root mean square error of the first-order polynomial warping function of less than 0.30 pixels was achieved.

For the radiometric calibration, a number of techniques were tested. The first set are physically based absolute atmospheric corrections where digital numbers (DNs) were converted to surface reflectances. However, a simpler empirical technique was eventually used as it was easier to employ and just as effective. This method uses a two-date density plot of DN values in which stable features in the images form a natural 'ridge' in the plot. A line was fitted along the ridge generating a simple linear relationship between the two images, which was used to match one date to the other. This approach has limitations if change constitutes a large portion of the image, or if there are significant seasonal differences between images. However, in this case it proved as helpful as a wide variety of other more complicated atmospheric correction methods. The methods tested and their results are presented in Song *et al.* (2000).

5. Change detection methodology

A common method of change detection is post-classification image comparison. One limitation of this method is that the accuracy of the change map typically will be at best the product of the accuracies of each individual classification for each date (Lambin and Strahler 1994). A method that circumvents this source of error is to analyse multidate images using a multi-temporal principal component technique (Fung and Le Drew 1987). This technique involves performing a principal component transformation using two dates of data to create new images that are uncorrelated with each other. The new principal component images are orthogonal to each other such that the first band of information contains the most variance in the original data, with each succeeding band containing increasingly less variance in the original data. Although this method is a useful data reduction technique, it can be difficult to associate physical scene characteristics with the individual components. Moreover, this type of analysis is scene dependent and therefore results between different dates may be difficult to interpret.

A multidate Tasseled Cap transformation is scene independent and has been shown to be successful in monitoring change (Fung 1990, Collins and Woodcock 1996). The Tasseled Cap transformation rotates TM data and creates three planes: Brightness (B), Greenness (G) and Wetness (W) (Crist and Cicone 1984). A substantial difference between the Tasseled Cap transformation and principal component analysis is that the former method employs fixed coefficients that can be applied to any scene across dates. The BGW bands are directly associated with physical scene attributes and therefore easily interpreted. The Brightness band is a weighted sum of all six reflective bands and can be interpreted as the overall brightness or albedo at the surface. The Greenness band primarily measures the contrast between the visible bands and near-infrared bands and is similar to a vegetation index. The Wetness band measures the difference between the weighted sum of the visible and near-infrared bands and the mid-infrared bands. As TM Bands 5 and 7 have been shown to be sensitive to moisture and water absorption, the Wetness band can be interpreted as a measure of soil and plant moisture.

In BGW space, different land-cover types occupy distinct spectral locations. Plotted in figure 1(*a*) and (*b*) are mean values from training site data for stable land-cover and land-use classes. The error bars represent one standard deviation from the mean for each class. A total of 809 training sites, consisting of 7807 pixels, were selected for 23 land-cover classes. The distribution of sites for each land-cover class is shown in table 1. The sites were selected based on visual interpretation of the images in the laboratory and from fieldwork. In the laboratory, an analyst familiar

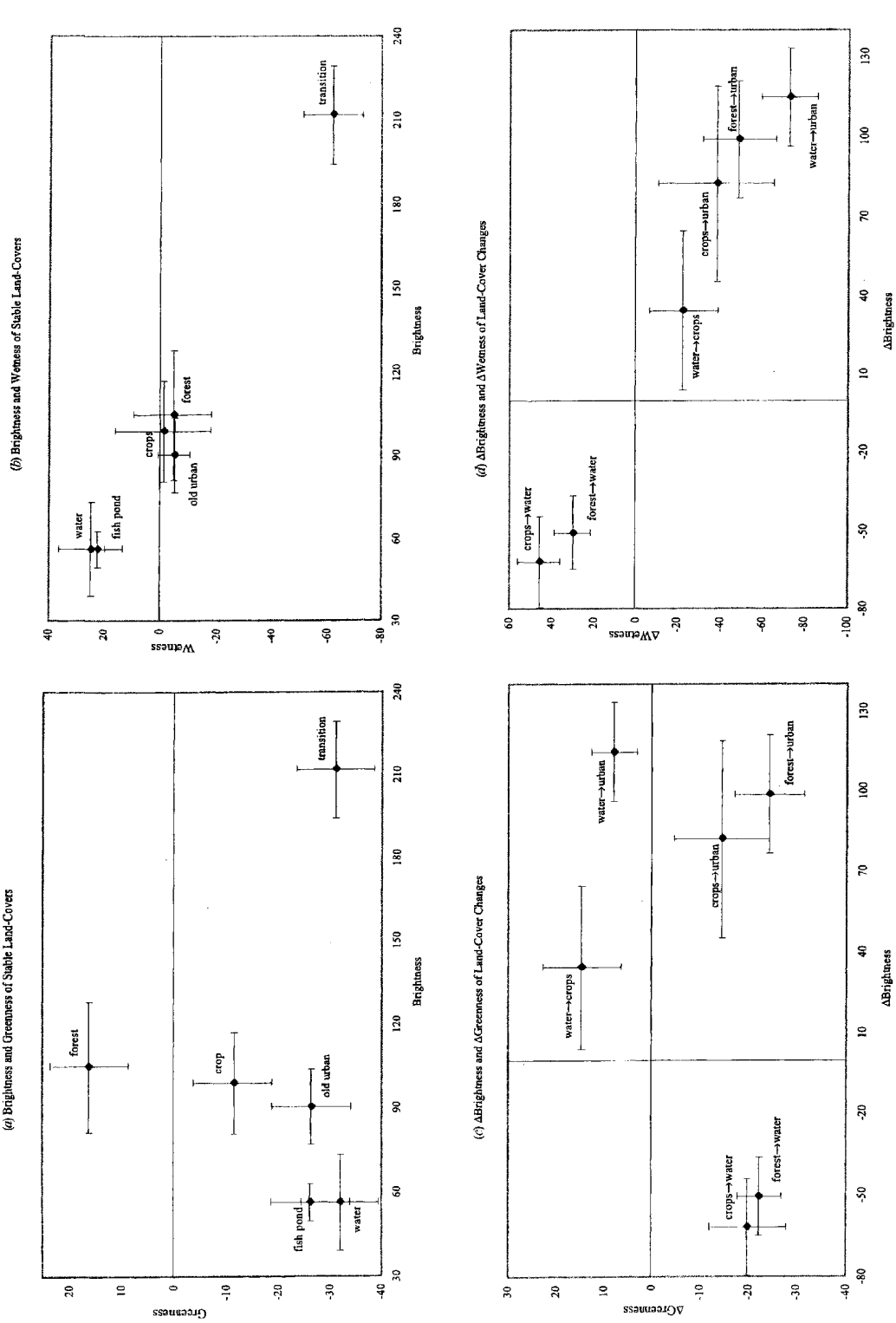

Figure 1. Mean Brightness, Greenness, Wetness, Δ Brightness, Δ Greenness and Δ Wetness values for stable and change land covers calculated from training data. Error bars represent one standard deviation away from mean. Distribution of sites for classes is shown in table 1.

Table 1. Land-covers and map classes for the PRD.*

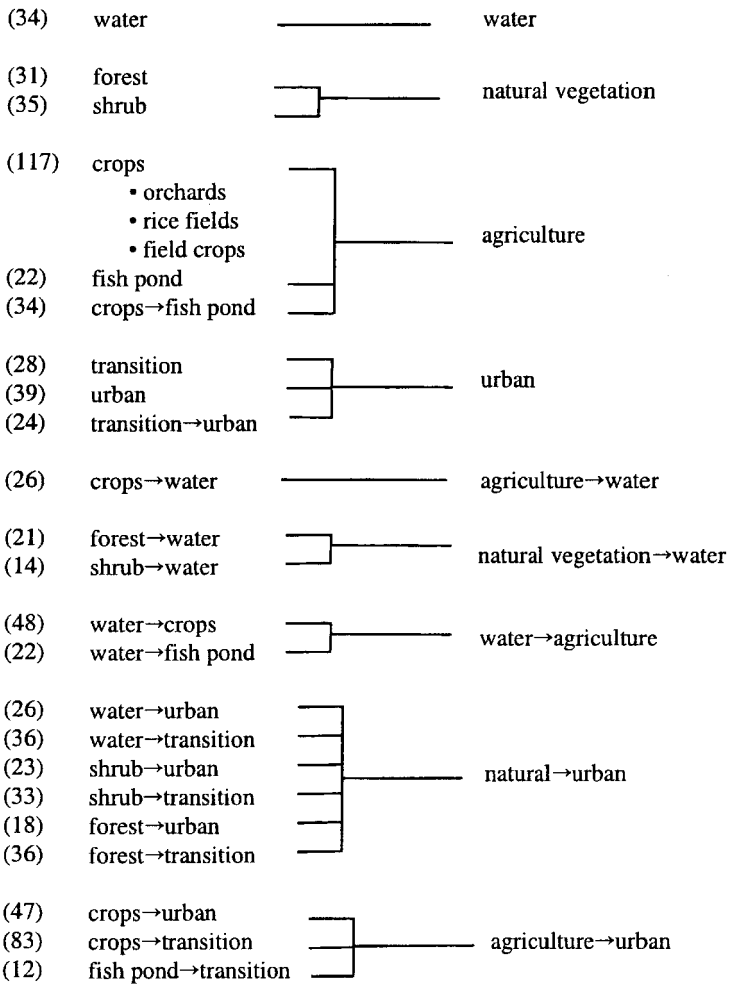

*Land-covers (centre) and the number of training sites for each category (left) which compromise the land-use classes (right).

with the region selected large areas (10–30 pixels) which were representative of the classes of interest. After this initial area selection, training sites within the areas were selected during fieldwork in China in February 1998. In the field, sites were georeferenced using a global positioning system (GPS) and digitized onto the image. Once in the field, some areas which had been selected in the laboratory were omitted from site selection due to limited access; it was simply not possible to have right of passage to all areas.

For the change classes, a two-step process was used to determine the land-use prior to land conversion. First, in the laboratory an analyst familiar with the region selected areas on the image where a substantial amount of land-use change had occurred. These areas were then analysed in greater detail to assess the type of land-use before and after land conversion. Sites within these areas were visited during

fieldwork in 1998. At the site, if a new urban area was located in the middle of an agricultural field, it was assumed that the land was previously used for agricultural purposes, and the site was labelled agriculture→urban. This conclusion was made and the change class labelled as such only when the prior land-use was evident from the surrounding geography. In areas where the prior land-use was not evident, interviews were carried out with local farmers and other land-users to obtain the land-use history of the site.

Old urban areas have features that generally exhibit high Brightness, low Wetness and low Greenness values while new urban, or transition, areas have the highest Brightness values. In contrast, water has high Wetness, low Brightness and low Greenness values. Although water and fish ponds are both water land-cover types, they exhibit some differences in their Greenness values. Crops and forest features have similar Wetness properties, but differ in their Greenness values. As land-cover changes over time, a change in reflectivity of the surface will exhibit corresponding changes in BGW values (figures 1(*c*) and (*d*)). Conversion of water to urban areas results in an increase in Greenness, an increase in Brightness and a decrease in Wetness. The change from crops to urban areas results in an increase in Brightness, a decrease in Greenness and a decrease in Wetness. As expected, the conversion of crops to water results in a decrease in Brightness, a decrease in Greenness and an increase in Wetness. Compared with new urban areas, croplands have a lower Brightness value, a higher Greenness value and a higher Wetness value. Conversely, new urban areas tend to be brighter, less green and less wet than agricultural land. Therefore, change from agricultural land to new urban areas will increase the Brightness, decrease the Greenness and decrease the Wetness values of BGW transforms.

In a six-dimensional space composed of BGW from the first date and a change in BGW between the two dates of imagery, a change vector can be mapped which traces the starting point of a pixel in date one, and its trajectory in date two. Because different land-cover types occupy distinct BGW space, it is important to know not only the magnitude and direction of change, but also the original location of each cover type in BGW space. BGW values were calculated separately for each date using standard Tasseled Cap coefficients (Crist and Cicone 1984), and then the values of the second date were subtracted from the first.

6. Classification process

We use a conceptual model to identify land-use change. Based on the idea that land-use classes are composed of component land-covers, we used land-cover as a 'bridge' between the images and the land-use classes. In essence, we attempt to map the component land-covers and then aggregate them into land-use and land-use change classes. In this context, the land-use classification process can be viewed as an exercise in disaggregation. First, the land-use and land-use change classes which are constructs relating to human activity or 'use' of land are disaggregated into their component physical manifestations, or land-covers. Secondly, the land-covers are disaggregated into their component spectral manifestations.

6.1. *Step 1: Define map classes*

The first step in our conceptual model is to define stable and change map classes of interest. The level of detail of the final map classes is dependent on end-user requirements. For our study, the socio-economic analysis will mainly focus on

the process of urbanization. Consequently, we are largely interested in two types of land conversion processes: (1) conversion from agriculture to urban areas, and (2) conversion from natural vegetation to urban areas. Four stable map classes are identified: water, urban areas, natural vegetation and agriculture. From the stable classes, we define change classes that will be of primary interest for the socio-economic analysis.

There may not be all combinations of change classes from the stable classes, as some change are unidirectional, and other change combinations simply do not occur. For example, agricultural land may be converted into urban areas, but it is unlikely that urban areas will be converted into agricultural land. However, agricultural land may be converted to forests through a tree replanting programme and forests can be converted for agricultural uses.

In defining the change classes, our interest is in the type of land that has been converted, not in the type of development that has occurred. It is irrelevant whether development results in the construction of a school, house or factory. Rather, the primary concern is how the land was used prior to conversion, and whether the land was used to generate an economic output. There is a higher opportunity cost of converting land with economic returns compared to converting land with no previous economic use. We assume that investors and land-users perform a formal or informal cost–benefit analysis of converting a parcel of land from its current use to another use before the conversion occurs.

Economically, there is little difference between a pond and a forest if neither is used to extract a resource or to generate economic revenue. If timber products are not extracted from the forest and the water from the pond is not used to irrigate crops or to raise fish, there is no economic opportunity cost associated with converting the pond or trees into a factory. The only characteristics that distinguish the pond from the forest are the differences in costs associated with preparing the land for development. However, if the pond were used to raise and harvest fish and the forest were used to extract wood products, the opportunity cost of converting these parcels of land would be the revenue generated from fish or timber products. For the land-user or investor to convert an economically viable parcel of land into another use, the new use of the land must generate more revenue or goods than the previous use.

Our change classes reflect this choice strategy. The five land-use change classes are: natural vegetation → water, agriculture → water, water → agriculture, natural → urban and agriculture → urban.

6.2. *Step 2: associating land-covers with land-uses*

After definition of the map classes, we identify 23 land-covers that can be associated with each of the stable and land-use change classes (table 1). The stable natural vegetation class includes both shrubs and forest. Therefore, a map class that includes natural vegetation is composed of the land-covers shrub and forest. The stable urban class includes two main points along the development continuum: (1) areas which have been cleared and are ready for construction to commence (transition), and (2) new urban areas, roads and the older sections of cities and towns. Transition areas are tracts of land which have been converted from natural vegetation, water or agriculture, but on which there has not been extensive construction. These parcels of land are essentially in 'transition' in that they are in the earlier stages of the development process. Sites that were transition in 1988 and either urban or transition

in 1996 are labelled stable urban areas. Sites that were not transition in 1988 but are transition in 1996 are labelled as one of the change classes. The stable agriculture class comprises crops and fish ponds. Crop types include orchards, rice fields and field crops.

A change in land-cover may not indicate a change in land-use. For example, field crops may be converted to fish ponds, which constitutes a change in land-cover. However, since the agriculture class does not differentiate among agriculture type, the crops → fish pond class includes conversion from orchards, rice fields or field crops to fish ponds and is a change in land-cover but not a change in land-use. Alternatively, a change in land-use may not constitute a change in land-cover. The water → agriculture class represents a specific region of the Delta where the water is being reclaimed for crop production and fish farms. This class includes water → fish pond and water → crops. The water → fish pond class is a change in land-use, but not a change in land-cover. Since both reservoirs and fish ponds are water bodies, differentiating between them can be difficult but is frequently possible because fish ponds differ in texture, tone and size from reservoirs. Anniversary date images may help alleviate some of the problems associated with changes due to crop phenology or the agricultural cycle that may show up as changes in land-cover but are not changes in land-use. However, anniversary date images are not always available and, even when they are available, differences in crop rotation, rainfall patterns and phenological maturation result in changes in spectral characteristics. Consequently, it cannot be assumed that changes in land-cover are indicative of changes in land-use, or that changes in land-use can be directly measured by changes in land-cover.

The natural vegetation → water class is defined as land that was previously either forest or shrubland and converted into a reservoir. The agriculture → water class includes different types of crops which were converted into reservoirs. The natural → urban class is composed of a number of land-covers, and includes both natural vegetation and water that were converted into urban or transition areas. The natural vegetation and water classes were aggregated into a single 'natural' land-use class to represent the conversion of land with no prior economic use. The rationale behind combining both land-covers into one land-use change class is that this represents conversion from a non-economic use to an economic use of the land. The conversion of these areas represents low or no opportunity cost of conversion. Therefore, we do not differentiate between conversion from water or forest to urban areas. The agriculture → urban class includes all types of agriculture that were converted into urban areas or transition areas. Together, the agriculture → urban and natural → urban classes account for urbanization in the Delta.

In general, land-use change is more difficult to map than land-cover change because the former requires an understanding of the anthropogenic use of the land and not simply land-cover characteristics. Agriculture is particularly difficult to characterize because of the spectral complexity of crop phenology and the variety of forms of agriculture.

6.3. *Step 3: multi-step classification*

The 23 stable and change land-covers identified in step 2 were used to classify land-use change. To characterize the complexity of agriculture and urban areas in the Delta, a multi-step classification procedure was used (figure 2).

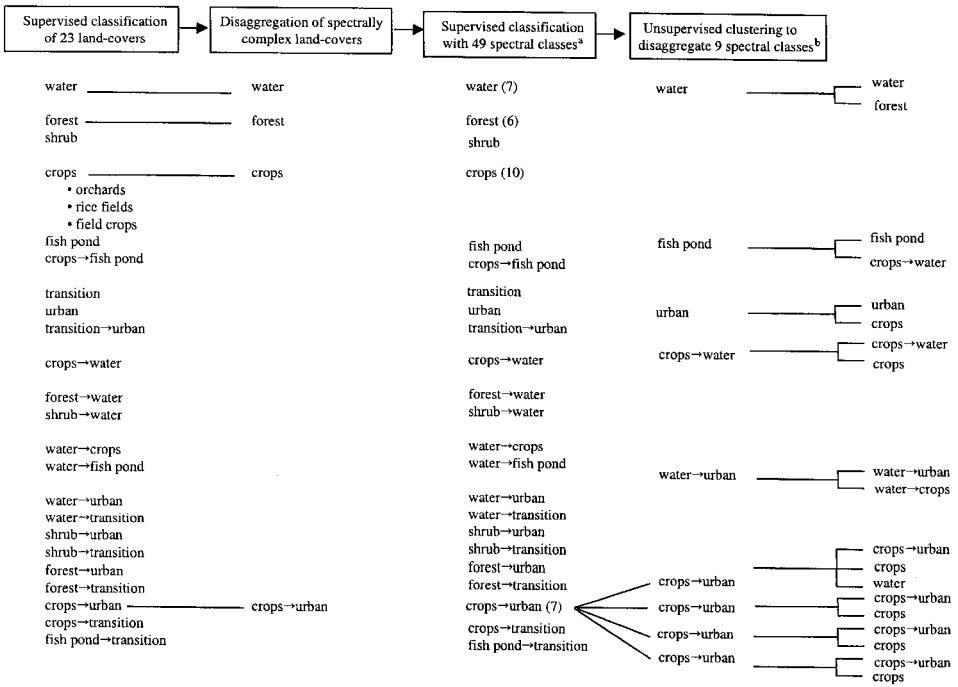

Figure 2. Schematic of multi-step classification. [a]Number of spectral classes in parentheses. [b]Each class was clustered into 10 spectral classes.

6.3.1. *Supervised classification*

We first performed a supervised maximum likelihood classification using a Bayesian classifier for the 23 land-covers (table 1). The inputs to the classifier were six bands of data: BGW for 1988, and changes in BGW (ΔB, ΔG, ΔW) between 1996 and 1988.

After the supervised classification, visual inspection of the results indicated that there was a large amount of misclassification in four of the classes: water, forest, crops and agriculture → urban. Much of the shadow in the forests was classified as water. Separation of the forest class into smaller classes would allow for better identification of forests in shadow versus in full sun. There was also confusion between crops and crops → urban. The cause of this confusion was probably the inherent variability within crops. The crops class includes orchards, field crops and rice fields, which are spectrally disparate types of agriculture. Therefore, a single training class of crops was too diverse accurately to train the classifier to identify disaggregated crop types.

6.3.2. *Spectral disaggregation: clustering of training sites*

The supervised classification using the 23 land-covers assumes each land-cover can be characterized spectrally by a single class. Experience has dictated that assumption is invalid for complex classes like crops which can include everything from inundated rice fields to sugar cane to orchards to fallow fields. One approach to disaggregating spectrally diverse classes is to use each training site as its own separate training class in the classification process, and then aggregate the appropriate spectral

classes into map classes after the classification. With 809 training sites, this approach was not feasible.

To disaggregate spectrally diverse land-covers, all the training sites for a single land-cover were clustered based on the Jeffries-Matusita (JM) distance, which measures the separability between training sites within a single land-cover (Richards 1995). The JM distance was calculated for all the sites for each class. Rather than training the data on a single forest class, calculating the JM distance disaggregated the forest class into smaller classes based on the spectral similarities of the sites.

Clustering was performed on the four classes identified from the supervised classification results as containing a large amount of misclassification. The single water class with 34 sites was clustered into seven spectral classes. It may seem unusual for water to be spectrally diverse. However, variations in turbidity levels, water depth and chlorophyll content all affect the spectral properties of water. Compared to a fresh water reservoir, water at the mouth of the Delta is particularly opaque due to discharge from the Pearl River. Therefore, it is expected that spectral reflectances will differ between the two water surfaces. The spectral characteristics of the crops class were particularly diverse owing to differences in crop types, phenology, plot sizes and soil attributes. A single crops class is inadequate in representing this variation, and therefore the 117 crops sites were separated into 10 spectral clusters. The original 31 forest sites were grouped into six clusters. Forests vary in tree species, crown structure, canopy density and topography. Forested mountains in the northern Delta are generally composed of dense pine or mixed species while bamboo and eucalyptus are more prevalent along riverbanks and in the southern Delta. The 47 agriculture→urban training sites were clustered into seven spectral classes to capture different starting points and different development trajectories of the urbanization process. These 30 spectral classes were combined with the original land-covers to create a dataset with 49 spectral classes which were used in a supervised maximum likelihood classification (figure 2).

6.4. *Image segmentation*

Once the classification was completed, visual inspection of the map indicated speckle through parts of the map. While previous misclassifications within classes exhibited a pattern (e.g. shadow of forests misclassified as water), the speckle was distributed throughout the map without a clear pattern. Rather than further separating the map classes, we used a multi-pass, region-based image segmentation algorithm to clean up some of the noisier classes and the problem of speckle.

The segmentation process uses the spatial component of an image to grow regions by merging neighbouring pixels into polygons, based on Euclidean distances (Woodcock and Harward 1992). One of the advantages of this technique is that it accounts for multiple scales within an image and yielded more accurate results than a single-pass filter. By detecting edges and specifying a minimum size of four pixels and a maximum polygon size of 1000×1000 pixels, the segmentation process produces polygons. The resulting polygons are labelled on the basis of the classes of the pixels inside each polygon using a simple plurality rule, which has the overall effect of removing individual isolated pixels, or speckle, from the map.

6.5. *Map editing*

Following the segmentation process, we conducted a final edit of the map. Some parts of the Delta that are exclusively agriculture were classified as urban while small

areas in the centre of the city of Guangzhou were classified as crops. Most of these areas that required further editing were limited to the immediate region around the city of Guangzhou and areas near the Delta. A possible cause of these geographic concentrations of misclassified areas is that atmospheric effects are not uniform throughout the image. Pollution in the city of Guangzhou creates a haze over the city, while the atmosphere near the coastal areas is clearer. This uneven distribution of pollution creates uneven atmospheric effects. Because a single radiometric calibration was applied to the entire image, there was no geographic correction of atmospheric effects. Therefore, editing was necessary to clean up some parts of the image. This involved relabelling approximately 5% of the entire image. Detailed knowledge and familiarity of the region was necessary for this type of editing.

7. Land-use change map and accuracy assessment

An example of the land-use change map is presented in figure 3. In an effort to offset the reduction of agricultural land to urbanization, a large area of the Delta has been reclaimed for banana, rice and sugar cane production, and fish farming. An example of this can be seen in the western section of the Delta in figure 3. Across the Delta, the magnitude of urban sprawl in the SEZ of Shenzhen and its environs is evident.

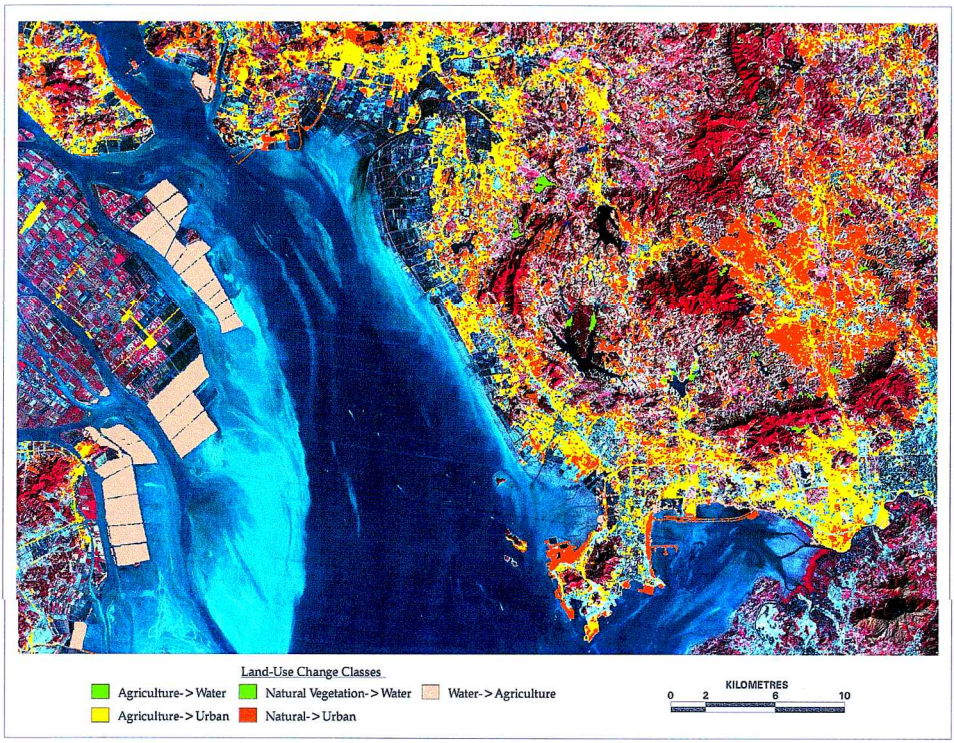

Figure 3. Land-use change in the Shenzhen region, 1988–1996. The background image is a full Landsat TM Band 4 acquired in 1995. New urban areas converted from agriculture lands are represented in green. New urban areas converted from natural vegetation or water are shown in yellow. New agricultural areas are shown in pink. The two new water classes (conversion from agriculture or natural vegetation) areaggregated for easier viewing and represented in magenta.

An accuracy assessment of the land-use change map was conducted using validation data entirely independent of the training data. Using a stratified random sampling scheme, 496 2×2 pixel sites were chosen. A stratified random sampling scheme was used to select the sites because the class sizes vary significantly, and a random sampling scheme may not have selected sites from all map classes in a well-distributed manner (Congalton 1991). During fieldwork in March and April 1999, 151 sites were analysed, while 345 sites were analysed in the laboratory at Boston University. In the laboratory, each site was viewed independently by at least two analysts. Only when both analysts agreed on the class type was the site labelled a particular class. If there was any discrepancy between two of the analysts, or if any analyst was unsure of the class for a site, the site was visited in the field. The initial screening of sites in the laboratory avoided the effort in the field of finding places where the answer was obvious, such as sites falling in the water in the Delta, in downtown Guangzhou, or in the forested mountains. Site assessments both in the laboratory and in the field were made without previous knowledge of the other analysts' choice of class type, nor of the final classification in the map. To assess the type of land-use prior to conversion, we relied primarily on interviews with land-users and farmers during fieldwork. In addition, we used similar procedures as those used for the training data: deductive reasoning in the field and analysis of the images in the laboratory.

Table 2 shows the confusion matrix of sites comparing the final map with ground observations. To calculate overall area-weighted accuracy of the map, the fraction of correctly labelled sites was weighted by the actual area proportion of each class (Card 1982). Table 3 shows the confusion matrix of sample sites weighted by the proportion of each class in the map. Area estimates were adjusted for each of the final classes after incorporating results from the field and the area-weighted estimates (table 4). The area-weighted classification accuracy is 93.5%.

After the field visits, the agriculture → water class lost almost half of its original area. Fourteen of the original 29 sites labelled as agriculture → water were identified as other classes in the field. Therefore, this class 'lost' 14 sites to these other classes. This left only 15 of the 29 sites labelled correctly as agriculture → water. However, the agriculture → water class also 'gained' eight new sites. That is, eight sites that were classified as natural → water in the map turned out to be actually agriculture → water sites. Therefore, the agriculture → water class 'gained' eight sites during the accuracy assessment. Consequently, the class agriculture → water 'lost' six sites. However, because this class represents only 0.06% of the total map, the adjusted area estimate is only -0.4% change. Conversely, the stable natural vegetation class on net 'lost' three sites which resulted in a change in area estimate of -5.71%. Because the natural vegetation class accounts for more than 46% of the map, loss or gain of a site from the accuracy assessment has large impacts on the area estimates for that class.

The user's accuracy of the two main classes of interest, agriculture → urban and natural → urban were 77.35% and 52.95%, respectively. Although the accuracy for the natural → urban class appears low, most of the confusion was with the agriculture → urban class. If the 'new urban' classes were aggregated, the accuracy would be 86.54%. Alternatively, the accuracy for the agriculture → water class is 51.72%, but if the 'new water' classes were aggregated, the accuracy would increase to 77.97%. More than one third of all sites in the agriculture → water class were misclassified. Fieldwork indicated that 11 of the 30 sites were actually fish ponds

Table 2. Confusion matrix comparing field assessments with map categories.*

	Ground data										
Map class	water	nat veg	ag	urban	ag→water	nat→water	water→ag	nat→urban	ag→urban	Sites	User's accuracy (%)
water	**49**									49	100.00
nat veg		**85**	6							91	93.41
ag		1	**109**	1					2	113	96.46
urban			2	**53**				1		56	94.64
ag→water	2		11		**15**	1				29	51.72
nat→water					8	**22**				30	73.33
water→ag							**24**			24	100.00
nat→urban	1	2	4					**27**	17	51	52.95
ag→urban			5	2				5	**41**	53	77.35
Totals										496	85.69

*The map categories are: water; natural vegetation from 1988 to 1996; agriculture from 1988 to 1996; urban from 1988 to 1996; conversion from agriculture (fish ponds and crops) to water; conversion from natural vegetation to water; conversion of water to agriculture; conversion of natural areas (natural vegetation and water) to urban; conversion from agriculture to urban. The user's accuracy refers to the probability of a map category on the map being the true class on the ground.

Table 3. Confusion matrix of true marginal proportions: sites weighted by proportion of each class in map.*

	Ground data										
Map class	water	nat veg	ag	urban	ag→water	nat→water	water→ag	nat→urban	ag→urban	Sites	Map prop.
water	**0.0776**									49	0.0776
nat veg		**0.4371**	0.0309							91	0.4680
ag		0.0031	**0.3382**	0.0031					0.0062	113	0.3506
urban			0.0008	**0.0219**				0.0004		56	0.0231
ag→water	0.0001		0.0004		**0.0006**					29	0.0011
nat→water					0.0001	**0.0002**				30	0.0003
water→ag							**0.0056**			24	0.0056
nat→urban	0.0005	0.0011	0.0022					**0.0147**	0.0092	51	0.0277
ag→urban			0.0043	0.0017				0.0043	**0.0355**	53	0.0458
True proportions	0.0782	0.4413	0.3768	0.0267	0.0007	0.0002	0.0056	0.0194	0.0509		
Producer's accuracy (%)	94.23	96.59	79.56	94.64	65.22	95.65	100.00	81.82	68.33	**93.14**	

*The cell probabilities are calculated as the proportion of sites identified in each class, weighted by the class proportion in the map. The true proportions are calculated as the sum of each column. The producer's accuracy is the probability of a particular class on the ground being correctly classified as that class on the map, and is calculated as a ratio of the cell probability of the corrected labelled sites to the true proportion of that class.

Table 4. Area estimates and adjusted area estimates of the final map classes.*

	Map estimate		Corrected map estimate		Net change
Class	(% of total area)	(km^2)	(% of total area)	(km^2)	(% of map estimate)
water	7.76	2094	7.82	2110	0.77
natural vegetation	46.80	12 626	44.13	11 906	−5.71
agriculture	35.06	9457	37.68	10 166	7.47
urban	2.31	624	2.67	720	15.58
agriculture → water	0.11	30	0.06	16	−0.46
natural vegetation → water	0.03	9	0.02	5	−0.33
water → agriculture	0.56	151	0.56	151	0.00
natural → urban	2.77	748	1.94	529	−29.97
agriculture → urban	4.58	1240	5.09	1376	11.14

*Totals may not sum to 100 due to rounding.

which had been converted from crops. Although this is a change in land-cover, it does not represent a change in land-use. This confusion highlights why it is more difficult to map land-use than land-cover using only satellite imagery.

8. Discussion

The high accuracy of the map was achieved by applying a conceptual model of identifying land-use change based on associated land-cover properties, using a multi-step classification process that accounted for the spectral complexity of many land-covers, and post-classification map editing. The multi-step classification allowed large classes to be disaggregated and clustered into finer spectral classes. A single-step classification would not have been successful in characterizing the complex nature of the landscape in the Delta.

The main source of confusion in the map is the agriculture class. The difficulty in characterizing the agriculture class is evident from the confusion matrix. Because the agriculture class is diverse and includes a variety of different agriculture types, there were a number of sites which were misclassified as change classes when they were actually stable agriculture. In the USA, most farms are large in size with monocrop production. In China, agriculture occurs at a much smaller scale, which can be likened to gardening with respect to the size of plots and the variety of crops produced. Multi-crop fields, terracing and small field sizes produce texture and tones that can be difficult to differentiate. Agricultural plots are generally small, less than an acre, but the plots of a village are usually adjacent to each other. The smaller plots and the variety of crop types within the plots creates heterogeneous surfaces which are more difficult to characterize than large area plots of a single monocrop. Cultivation of vegetables, fish ponds, and fruit orchards often abut each other, giving images a heterogeneous texture that is difficult to characterize.

Conversion of agriculture occurs on a few different scales. An increase in the income of some farmers has permitted the refurbishing of old and construction of new homes. The use of new materials often creates a change in spectral signal distinct from the surrounding agriculture. New homes constructed by farmers generally are built with brick. After rice has been harvested, rice fields are essentially bare plots of soil, which spectrally look similar to land which has been cleared for construction of new buildings. Only when rice fields maintain a high level of moisture are they

spectrally distinct from bright, dry soils. Therefore, the phenological and planting cycles of rice can be confused with transition areas.

There is significant confusion between the two urbanization classes, agriculture → urban and natural → urban. The natural → urban class lost one third of its total area to the agriculture → urban class. In this study, the stability of the area estimates is closely related to the level of detail in the classification. If no distinction were made between types of urbanization, then the overall accuracy of the map would be higher.

The results indicate that the conceptual model was useful in guiding the identification of land-use from land-cover features. Without distinguishing between land-cover and land-use change, some changes would have been misidentified as land-use changes when they were only changes in land-cover. Similarly, changes in land-use that did not create a change in land-cover would have been misclassified as stable land-use. There are numerous stages and types of urban development in the Delta, and although it is possible to discern an old urban area from a recently cleared construction site, it is difficult to differentiate between newer buildings and different stages of construction. Therefore, it was necessary to include different stages in the development continuum to better capture the urban development phenology.

Between the period 1988–1996, the Pearl River Delta experienced a scale of land conversion unprecedented in the history of the country; approximately 1905 km^2 of land was converted to urban uses during this period, an increase in urbanization of 364%. From an estimated 720 km^2 of urban area in 1988, or 2.67% of the study area, the Delta's urban land increased to over 2625 km^2 by 1996. Urban areas now comprise almost 10% of the study area. While approximately a quarter of the new urban areas were previously natural vegetation or water, most were converted from farmland, approximately 1376 km^2. The central and provincial governments recognize the threat of declining agricultural land, and have supported initiatives to reclaim part of the Delta for agriculture. Indeed, approximately 151 km^2 of the Delta's water areas were converted into farmland. However, this increase in agricultural land offsets the loss in agricultural land by only 11%. Yet, without a rigorous study of differences in agricultural yield, it is difficult to assess the impacts of agricultural land loss on food production and food prices.

9. Conclusions

The results indicate our conceptual model of land-use classes, being composed of spectrally diverse land-covers, provides a good framework with which to infer land-use change from land-cover characteristics. The multi-step classification algorithm was necessary to capture the complexity of the landscape, and to map the changes with a high degree of accuracy. An accuracy assessment was essential to identify problems in the map and to improve area estimates for each class. Particularly for a project in which one of the objectives is to obtain area estimates by land-use class, an accuracy assessment is vital. Moreover, an accuracy assessment is essential in identification of and correction for errors in misclassifying land-use versus land-cover changes.

The rate of urbanization and land conversion is unprecedented. Historically, the Pearl River Delta has been a region of relatively little land conversion and population growth. Land-use patterns and agricultural practices in much of the Delta have remained constant for hundreds of years. Given the economic growth that has directly improved the living standards of most citizens in the Delta, urbanization rates of more than 300% between 1988 and 1996 is not unexpected, but still

impressive. However, since most of the conversion of land is from agriculture, rapid urban development has potentially serious implications for a number of issues, including regional food supply and biogeochemistry.

Acknowledgement

This research was supported by NASA grant NAG5-6214.

References

Campbell, J. B., 1983, *Mapping the Land* (Washington, D.C.: AAG).

Card, D. H., 1982, Using known map category marginal frequencies to improve estimates of thematic map accuracy. *Photogrammetric Engineering and Remote Sensing*, **48**, 431–439.

Chu, D. K. Y., 1998, Synthesis of economic reforms and open policy. In *Guangdong: Survey of a Province Undergoing Rapid Change*, edited by Y. M. Yeung and D. K. Y. Chu (Hong Kong: The Chinese University Press), pp. 485–504.

Collins, J. B., and Woodcock, C. E., 1994, Change detection using the Gramm-Schmidt transformation applied to mapping forest mortality. *Remote Sensing of Environment*, **50**, 267–279.

Collins, J. B., and Woodcock, C. E., 1996, As assessment of several linear change detection techniques for mapping forest mortality using multitemporal Landsat TM data. *Remote Sensing of Environment*, **56**, 66–77.

Congalton, R. G., 1991, A review of assessing the accuracy of classification of remotely sensed data. *Remote Sensing of Environment*, **37**, 35–46.

Coppin, P. R., and Bauer, M. E., 1994, Processing of multitemporal Landsat TM imagery to optimize extraction of forest cover change features. *IEEE Transactions on Geoscience and Remote Sensing*, **32**, 918–927.

Crist, E. P., and Cicone, R. C., 1984, A physically-based transformation of Thematic Mapper data—The TM Tasseled Cap. *IEEE Transactions on Geoscience and Remote Sensing*, **22**, 256–263.

Dimyati, M., Mizuno, K., Kobayashi, S., and Kitamura, T., 1996, An analysis of land use/cover change using the combination of MSS Landsat and land use map—a case study in Yogyakarta, Indonesia. *International Journal of Remote Sensing*, **17**, 931–944.

Forster, B. C., 1993, Coefficient of variation as a measure of urban spatial attributes, using SPOT HRV and Landsat TM data. *International Journal of Remote Sensing*, **14**, 2403–2409.

Fung, T., 1990, An assessment of TM imagery for land-cover change detection. *IEEE Transactions on Geoscience and Remote Sensing*, **28**, 681–684.

Fung, T., and Le Drew, E., 1987, Application of principal components analysis to change detection. *Photogrammetric Engineering and Remote Sensing*, **53**, 1649–1658.

Gong, P., and Howarth, P. J., 1990, The use of structural information for improving land-cover classification accuracies at the rural–urban fringe. *Photogrammetric Engineering and Remote Sensing*, **56**, 67–73.

Gopal, S., and Woodcock, C. E., 1996, Remote sensing of forest change using artificial neural networks. *IEEE Transactions on Geoscience and Remote Sensing*, **34**, 398–404.

Green, K., Kempka, D., and Lackey, L., 1994, Using remote sensing to detect and monitor land-cover and land-use change. *Photogrammetric Engineering and Remote Sensing*, **60**, 331–337.

Guangdong Statistical Bureau, 1998, *Statistical Yearbook of Guangdong* (Beijing: China Statistical Publishing House).

Guangdong Statistical Bureau, various years, *Statistical Yearbook of Guangdong* (Beijing: China Statistical Publishing House).

Haack, B., Bryant, N., and Adams, S., 1987, An assessment of Landsat MSS and TM data for urban and near-urban land-cover digital classification. *Remote Sensing of Environment*, **21**, 201–213.

Heikkonen, J., and Varfis, A., 1998, Land cover/land use classification of urban areas: a remote sensing approach. *International Journal of Pattern Recognition and Artificial Intelligence*, **12**, 475–489.

HOWARTH, P. J., and BOASSON, E., 1983, Landsat digital enhancements for change detection in urban environments. *Remote Sensing of Environment*, **13**, 149–160.

JENSEN, J. R., and TOLL, D. L., 1982, Detecting residential land-use development at the urban fringe. *Photogrammetric Engineering and Remote Sensing*, **48**, 629–643.

KHORRAM, S., BROCKHAUS, J. A., and CHESHIRE, H. M., 1987, Comparison of Landsat MSS and TM data for urban land-use classification. *IEEE Transactions on Geoscience and Remote Sensing*, **25**, 238–243.

LAMBIN, E. F., and STRAHLER, A. H., 1994, Change vector analysis in multitemporal space: a tool to detect and categorize land-cover change processes using high temporal-resolution satellite data. *Remote Sensing of Environment*, **48**, 231–244.

LI, X., and YEH, A. G. O., 1998, Principal component analysis of stacked multi-temporal images for the monitoring of rapid urban expansion in the Pearl River Delta. *International Journal of Remote Sensing*, **19**, 1501–1518.

MACLEOD, R. D., and CONGALTON, R. G., 1998, A quantitative comparison of change-detection algorithms for monitoring eelgrass from remotely sensed data. *Photogrammetric Engineering and Remote Sensing*, **64**, 207–216.

MØLLER-JENSEN, L., 1990, Knowledge-based classification of an urban area using texture and context information in Landsat-TM imagery. *Photogrammetric Engineering and Remote Sensing*, **56**, 899–904.

NING, C., 1991, Price reform and the future model in the Special Economic Zones of China. *Chinese Economic Studies*, **24**, 76–92.

PAX LENNEY, M., WOODCOCK, C. E., COLLINS, J. B., and HAMDI, H., 1996, The status of agricultural lands in Egypt: the use of multitemporal NDVI features derived from Landsat TM. *Remote Sensing of Environment*, **56**, 8–20.

RICHARDS, J. A., 1995, *Remote Sensing Digital Image Analysis* (New York: Springer-Verlag), p. 250.

RIDD, M. K., and LIU, J., 1998, A comparison of four algorithms for change detection in an urban environment. *Remote Sensing of Environment*, **63**, 95–100.

SICULAR, T., 1985, China's grain and meat economy: recent development and implications for trade. *American Journal of Agricultural Economics*, **67**, 1055–1062.

SINGH, A., 1989, Digital change detection techniques using remotely-sensed data. *International Journal of Remote Sensing*, **10**, 989–1003.

SKOLE, D. L., CHOMENTOWSKI, W. H., SALAS, W. A., and NOBRE, A. D., 1994, Physical and human dimensions of tropical deforestation in the Brazilian Amazon. *Bioscience*, **44**, 314–322.

SMIL, V., 1993, *China's Environmental Crisis* (Armonk, N.Y: M. E. Sharpe).

SMIL, V., 1995, Who will feed China? *The China Quarterly*, **143**, 801–813.

SONG, C., WOODCOCK, C. E., SETO, K. C., PAX LENNEY, M., and MACOMBER, S. A., 2000, An evaluation of the effects of several atmospheric correction algorithms on classification and change detection using Landsat TM data. *Remote Sensing of Environment*.

WOODCOCK, C. E., and HARWARD, J., 1992, Nested-hierarchical scene models and image segmentation. *International Journal of Remote Sensing*, **13**, 3167–3187.

WOODCOCK, C. E., and STRAHLER, A. H., 1987, The factor of scale in remote sensing. *Remote Sensing of Environment*, **21**, 311–332.

WORLD RESOURCES INSTITUTE, 1994, *World Resources 1994–1995* (Oxford: Oxford University Press).

WU, C.-T., 1989, The special economic zones and the development of the Zhujiang Delta area. *Asian Geographer*, **8**, 71–87.